PHYSICAL REVIEW D VOLUME 27, NUMBER 8 15 APRIL 1983

Planar rotor: The θ-vacuum structure, and some approximate methods in quantum mechanics

M. Asorey
Departamento de Física Teórica, Universidad de Zaragoza, Zaragoza, Spain

J. G. Esteve and A. F. Pacheco
Departamento de Física Nuclear, Universidad de Zaragoza, Zaragoza, Spain

(Received 15 November 1982)

The quantum planar rotor is chosen as a model to test different approximate techniques, emphasizing the analogies between this simple system and the non-Abelian quantum gauge field theories (instantons, θ vacuum, etc.). In particular, variational and perturbative methods, path-integral techniques, and Monte Carlo simulations are applied. It is pointed out that the maximal destructive interference between instantons takes place in the θ-vacuum realization of the interacting rotor system with $\theta=1/2$, where the tunneling effects are shown to be severely diminished.

I. INTRODUCTION

In the past few years we have seen a marked increase of interest in connection with the study of approximate, nonperturbative methods in quantum field theories. These methods are particularly important for the study of strong-coupling field theories, quark confinement in QCD, computation of hadron masses and glueball masses in the context of the θ vacuum of Yang-Mills theories, the solution of the U(1) problem, etc.[1] Roughly speaking, we may divide these techniques into two big groups, those inspired in semiclassical approximations[2,3] (solitons, instantons, etc.) and those based on the lattice strategy[4] (mean field, renormalization group, Monte Carlo simulations, etc.). These methods have been devised to attack a quantum field theory where the degree of quantitative accuracy one attains is usually unknown, and very often the methods are unfamiliar to the rest of the physics community. That is why we consider it interesting to apply them to a simple problem of quantum mechanics in order to observe in detail their structure and numerical precision.

We have chosen the plane rotor because from the theoretical point of view it presents many analogies with the non-Abelian gauge theories. In particular, because of its topology it possesses different quantum realizations which imply the existence of the θ-vacuum phenomenon; furthermore, this system under certain interactions allows the appearance of instantons. On the other hand, this simple model simulates some quite interesting physical situations such as the spectrum of certain molecules,[5] and the motion of the electrons in a circular SQUID.[6]

The plan of the paper is as follows. In Sec. II we study the free rotor quantum problem from both perspectives, the Hamiltonian and the path-integral one. In both approaches an exact description of the spectrum is attained, corresponding to each θ-vacuum realization (ϵ vacuum in our notation); for $\theta=\frac{1}{2}$ one observes the existence of a degeneracy in the ground state and a phase transition. The origin of the θ-vacuum phenomena is discussed in detail. In the path-integral formalism it comes from the contribution of closed trajectories with nonzero winding number. In the Hamiltonian perspective, it is the existence of different quantum Hamiltonians corresponding to the same classical dynamics that is responsible for it. As is known, from an experimental point of view the θ phenomenon may be implemented[6] by confining a magnetic flux within the ring of the rotor. In Sec. III the "charged" rotor is influenced by an external uniform electric field, which leads to the Matthieu problem with its well-known solutions. Section IV is entirely devoted to the analysis of the performances of different approximate standard techniques to get information about the problem addressed in Sec. III. Specifically, we have considered a variational Tamm-Dancoff method, the standard perturbation theory, and the self-consistent linearization, Hartree-type method. The semiclassical approach to that problem is analyzed in Sec. V by calculating the multi-instanton contributions in a dilute-gas regime. In Sec. VI we approximate the path integral of the in-

teracting system by making discrete the temporal coordinate and performing Monte Carlo simulations. In Secs. III–VI our analysis is restricted to the $\theta=0$ case. In Sec. VII we study the system in interaction with an external uniform electric field strength in an arbitrary θ-vacuum realization, by using semiclassical (instantons) and variational tools. Finally, in Sec. VIII our results and conclusions are collected.

II. THE FREE PLANAR ROTOR

A. Canonical quantization approach

Let us consider the dynamical system associated with a free nonrelativistic particle constrained to move in a circumference S^1 of unit radius. The corresponding classical Lagrangian is

$$L=\tfrac{1}{2}\dot{\theta}^2 , \tag{2.1}$$

where θ is the angle ($0\leq\theta\leq 2\pi$) and the mass of the particle is supposed to be unity.

The corresponding quantum system is defined in $L^2(S^1,d\theta)$ by the Hamiltonian ($\hbar=1$)

$$H=-\frac{1}{2}\frac{d^2}{d\theta^2} \tag{2.2}$$

acting on differentiable functions ψ of S^1, vanishing in a neighbor set of 0 (or 2π). The self-adjoint extension of H to be considered depends on the boundary conditions imposed at 0 and 2π, and since the particle moves freely on S^1 the boundary conditions are periodic; then the corresponding extension H_0 of H is defined in

$$D(H_0)=\{f:S^1\rightarrow C;\ f \text{ absolutely continuous};\ f(0)=f(2\pi)\} . \tag{2.3}$$

The classical equation of motion corresponding to the Lagrangian (2.1),

$$\ddot{\theta}=0 , \tag{2.4}$$

is also generated by the Lagrangian

$$L_\epsilon=\tfrac{1}{2}(\dot{\theta}+\epsilon)^2-\tfrac{1}{2}\epsilon^2 . \tag{2.5}$$

However, the quantum Hamiltonian associated with (2.5) defined by

$$H_\epsilon=-\frac{1}{2}\left[\frac{d}{d\theta}-i\epsilon\right]^2 \tag{2.6}$$

in the domain $D(H_0)$ has a different spectrum than H_0 if ϵ is not an integer constant. Therefore, there are inequivalent quantum realizations of the same classical system.

The expressions (2.5) and (2.6) can also be considered, respectively, as the classical Lagrangian and quantum Hamiltonian of a charged particle ($e=1$) moving in S^1 under the action of an electromagnetic field A_μ tangent to S^1 with constant norm ϵ and pointing in the anticlockwise direction as we can see in Fig. 1.

Such an electromagnetic field corresponds to a physical situation where an external magnetic field $\vec{B}$ is confined in a region S encircled by S^1 with magnetic flux

$$\phi=\int_S \vec{B}\cdot d\vec{S}=\int_{S^1}\vec{A}\cdot d\vec{l}=2\pi\epsilon . \tag{2.7}$$

As is well known, since the relevant classical quantities are the values of the electric E and magnetic B fields in S^1, the classical equation of motion corresponding to the above physical situations (2.1) and (2.5) are the same. However, since the spectra of (2.2) and (2.6) are different if ϵ is not an integer number, both situations are different from the quantum point of view; this shows that the relevant quantum quantities are the electromagnetic fields (up to equivalences) rather than the magnetic and electric fields, as is well known from the Aharonov-Bohm effect.[7]

On the other hand, the quantum system described by (2.6) can be simulated from the free system (2.2) by modifying the boundary conditions at a point of S^1. Let H_0^ϵ be the self-adjoint extension of the differential operator (2.2) defined in the domain

$$D(H_0^\epsilon)=\{f:S^1\rightarrow C;f \text{ absolutely continuous};\ f(0)=e^{-i2\pi\epsilon}f(2\pi)\} , \tag{2.8}$$

which corresponds to imposing quasiperiodic boun-

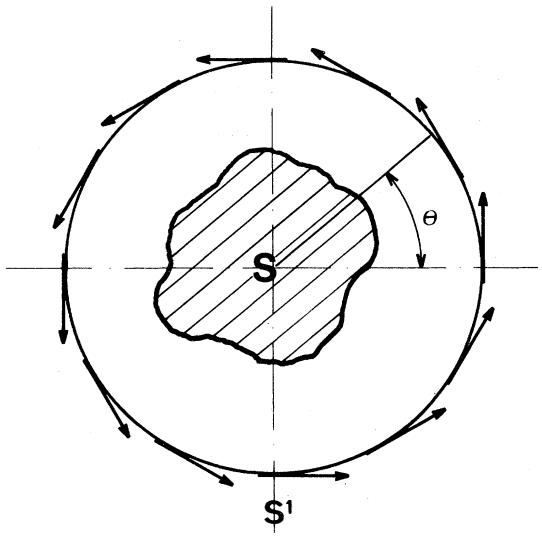

FIG. 1. Illustration of the Aharonov-Bohm effect. S is the region with a nonzero magnetic field strength.

dary conditions at $\theta=0$. Then, the unitary operator

$$T:L^2(S^1,d\theta)\to L^2(S^1,d\theta)\ ,$$

given by

$$T\psi(\theta)=e^{-i\epsilon\theta}\psi(\theta)\ , \tag{2.9}$$

verifies that

$$T^{-1}H_0^{\epsilon}T=H_{\epsilon}\ . \tag{2.10}$$

Thus, the physical systems described by H_ϵ and H_0^ϵ are equivalent (note that H_0^ϵ and $H_0^{\epsilon+n}$ with n an integer are the same operators, therefore the different dynamics are parametrized by $\epsilon\in[0,1)$). The equivalence (2.10) has caused the authors of Ref. 8 to error because they assume that the change of the electromagnetic fields implies automatically a change of the boundary conditions which leaves the system equivalent to the free case; then they claimed against the existence of the Aharonov-Bohm effect.

However, the boundary conditions at $\theta=0$ have nothing to do with electromagnetic fields but with local physical manipulations at this point of the space. In the absence of such local manipulations the boundary conditions are always periodic and the action of the electromagnetic fields does not change them since it only changes the dynamics of the particle.[9]

The solution of the spectral problem for the Hamiltonian considered above is completely straightforward. The eigenstates and eigenvalues of H_ϵ in $D(H_0)$ are given by

$$\varphi_n=\frac{1}{\sqrt{2\pi}}e^{in\theta}\ , \tag{2.11}$$

$$E_n^{\epsilon}=\tfrac{1}{2}(n-\epsilon)^2\ , \tag{2.12}$$

where $n=0,\pm1,\pm2,\ldots$ and where the expression (2.12) shows explicitly that the spectra of H_ϵ and $H_{\epsilon+r}$ are the same provided that r is an integer. On the other hand, the eigenstates and eigenvalues of H_0^ϵ in $D(H_0^\epsilon)$ are given by

$$\varphi_n^{\epsilon}(\theta)=\frac{1}{\sqrt{2\pi}}e^{i(n-\epsilon)\theta}\ , \tag{2.13}$$

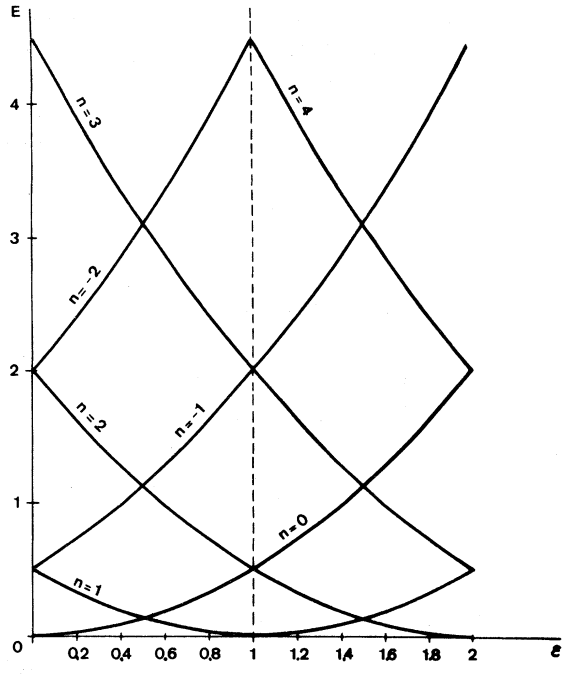

FIG. 2. Energy levels for the free rotor.

$$E_n'^{\epsilon}=\tfrac{1}{2}(n-\epsilon)^2\ , \tag{2.14}$$

where $n=0,\pm1,\pm2,\ldots$.

The equivalence of H_0^ϵ and H_ϵ is shown by the fact that $E_n'^{\epsilon}=E_n^{\epsilon}$ and $\varphi_n(\theta)=T\varphi_n(\theta)$. In this second approach, the domains $D(H_0^\epsilon)$ depend on $\epsilon\in[0,1)$ and the eigenstates (2.13) also depend on it, which for the ground state is known as the ϵ-vacuum dependence.

It should be noted that the ϵ dependence of the ground-state energy plotted in Fig. 2 shows the existence of a "second-order phase transition" at $\epsilon=\frac{1}{2}$ where the ground state is degenerate (minimax theorem does not apply to H_0 because of the existence of boundary terms). The above results have recently been confirmed in the laboratory by the authors of Ref. 6 using a circular SQUID.

B. Path-integral approach

The quantum Euclidean propagator $K_E(T;\{\theta\},\{\theta'\})$ corresponding to the evolution operator $e^{-H_\epsilon T}$ is given by

$$K_E(T;\{\theta\},\{\theta'\})=\langle\{\theta'\}\,|\,e^{-TH_\epsilon}\,|\,\{\theta\}\rangle=\sum_{n=-\infty}^{+\infty}e^{-E_nT}\varphi_n^*(\{\theta'\})\varphi_n(\{\theta\})\ , \tag{2.15}$$

where $|\,\{\theta\}\rangle$ and $|\,\{\theta'\}\rangle$ are position eigenstates and $\{\theta\}$ denotes the class of θ modulo 2π, φ_n and E_n being the eigenfunctions and eigenvalues given by (2.11) and (2.12). The propagator K_E admits also a path-integral

representation[10] given by

$$K_E(T;\{\theta\},\{\theta'\})=N\int_{\{\theta(0)\}=\{\theta\}}^{\{\theta(T)\}=\{\theta'\}}\prod_t d\theta(t)\exp\left[\int_0^T L_E(\dot\theta,\epsilon)dt\right], \tag{2.16}$$

where L_E is the Euclidean Lagrangian and N is a normalization factor,

$$L_E(\dot\theta,\epsilon)=-(\tfrac{1}{2}\dot\theta^2+i\epsilon\dot\theta)\,. \tag{2.17}$$

Then

$$K_E(T;\{0\},\{0\})=N\int_{\{\theta(0)\}=\{0\}}^{\{\theta(T)\}=\{0\}}\prod_t d\theta(t)\exp\left[-\int_0^T\frac{\dot\theta^2}{2}dt\right]e^{-i\epsilon\chi(\theta(t))2\pi}, \tag{2.18}$$

where $\chi(\theta(t))$ is the winding number of the path $\theta(t)$, i.e., the net number of times $\theta(t)$ rounds S^1 clockwise. Therefore, the functional integral splits in path sectors parametrized by the winding number χ:m,

$$K_E(T;\{0\},\{0\})=\sum_{m=-\infty}^{+\infty}N\int_{\theta(0)=0}^{\theta(T)=2m\pi}\prod_t d\theta(t)\exp\left[-\int_0^T\frac{\dot\theta^2}{2}dt\right]e^{-i\epsilon m2\pi}\,.$$

Since

$$N\int_{\theta(0)=0}^{\theta(T)=2m\pi}\prod_t d\theta(t)\exp\left[-\int_0^T\frac{\dot\theta^2}{2}d\theta\right]=\frac{1}{\sqrt{2\pi T}}e^{-2\pi^2m^2/T}, \tag{2.19}$$

then

$$K_E(T;\{0\},\{0\})=\frac{1}{\sqrt{2\pi T}}\sum_{m=-\infty}^{+\infty}\exp\{-[2(\pi m)^2/T]-i2\pi\epsilon m\}\,. \tag{2.20}$$

By making use of the Poisson formula

$$\sum_{m=-\infty}^{+\infty}f(m)=\sum_{m=-\infty}^{+\infty}\int_{-\infty}^{+\infty}f(t)e^{-2\pi imt}dt \tag{2.21}$$

applied to the function $f(x)=\exp[-(x-\epsilon)^2T/2]$, (2.20) leads to (2.14).

Thus, in this free case, the path-integral method provides us with the exact solution of the spectral problem of H_ϵ. This method also stresses the appearance of ϵ sectors in terms of the existence of path sectors with different topological winding numbers; this result also holds when there is an additional potential term in the Lagrangian (2.5).

III. THE PLANAR ROTOR IN A UNIFORM ELECTRIC FIELD

Let us now consider the action of a uniform electric field with field strength λ on a nonrelativistic electron ($e=1$) constrained to move in S^1. The quantum Hamiltonian corresponding to this interacting planar rotor is given by the self-adjoint extension of

$$H=-\frac{1}{2}\frac{d^2}{d\theta^2}+\lambda\cos\theta \tag{3.1}$$

defined in the domain $D(H_0)$. The spectral equation of H,

$$H\psi=E\psi\,,$$

is a Matthieu-type equation.

There are only two kinds of solutions of (3.2) in $D(H_0)$. In fact, only the solutions a_{2r} and b_{2r} of the Matthieu equation satisfy the boundary conditions

$$\psi(0)=\psi(2\pi)$$

and

$$\left.\frac{d}{d\theta}\psi\right|_0=\left.\frac{d}{d\theta}\psi\right|_\pi\,.$$

The asymptotic behavior (for small λ) of the lowest eigenvalues of H is given by[11]

$$E_{a_0}(\lambda)=-\lambda^2+\tfrac{7}{4}\lambda^4-\tfrac{58}{9}\lambda^6+\tfrac{68\,687}{2304}\lambda^8+\cdots\,, \tag{3.2a}$$

$$E_{b_2}(\lambda)=\tfrac{1}{2}-\tfrac{1}{6}\lambda^2+\tfrac{1}{432}\lambda^4+\tfrac{1\,002\,401}{155\,520}\lambda^6+\cdots\,. \tag{3.2b}$$

The corresponding expressions (for big λ) are

$$E_{a_0}=-\lambda+\tfrac{1}{2}\sqrt{\lambda}-\frac{1}{32}-\frac{1}{2^9\sqrt{\lambda}}-\frac{3}{2^{13}\lambda}+\cdots\,, \tag{3.3a}$$

$$E_{b_2} = -\lambda + \tfrac{3}{2}\sqrt{\lambda} - \frac{5}{32} - \frac{9}{2^9\sqrt{\lambda}} - \frac{45}{2^{13}\lambda} + \cdots . \tag{3.3b}$$

The λ dependence of the ground-state energy given by (3.2a) and (3.3a) is graphically displayed in Fig. 3 (see also column four of Table I). The precision obtained from this method by choosing $\lambda=0.4$ as the matching point between the two complementary asymptotic expansions (3.2a) are (3.3a) is remarkable.

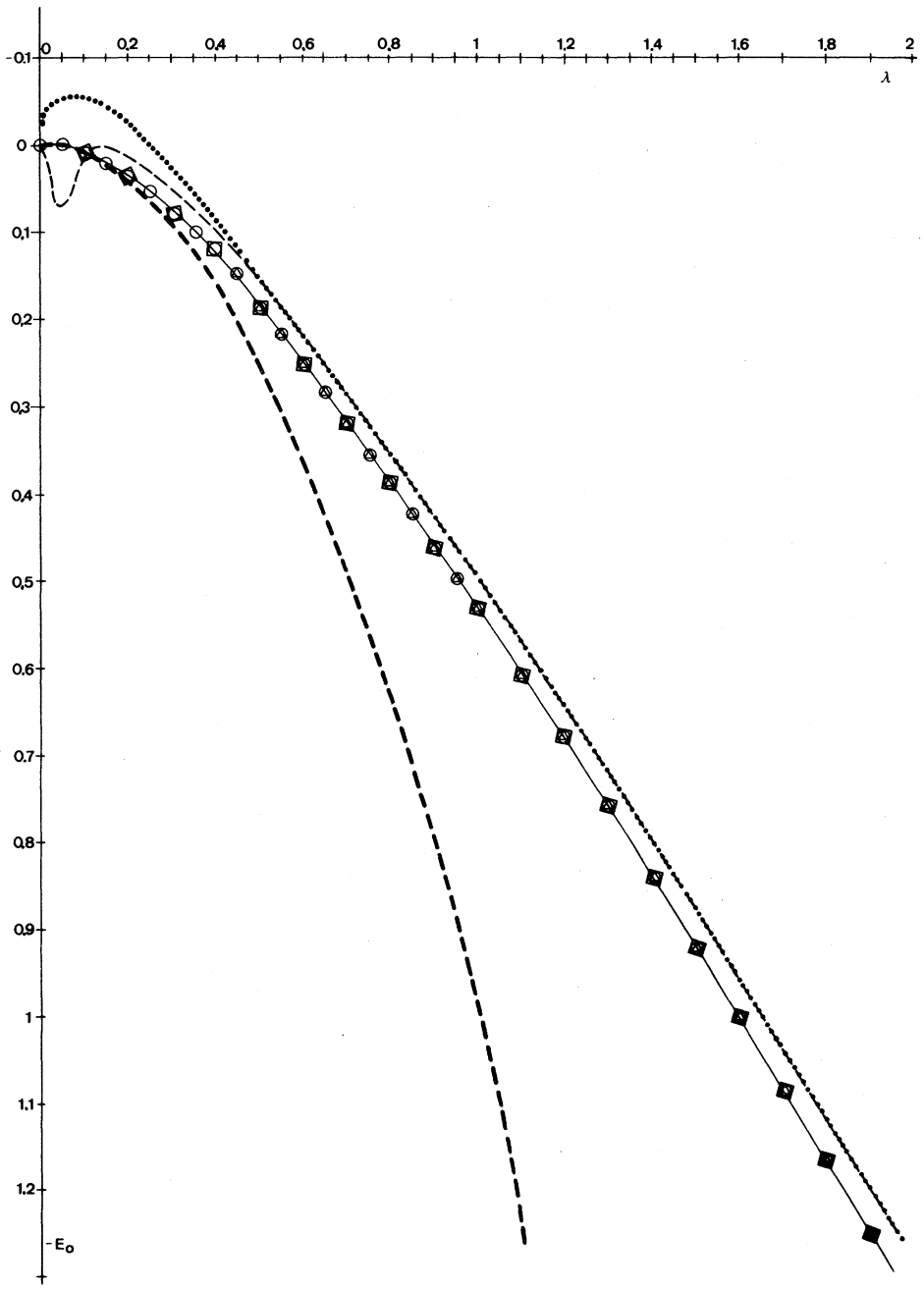

FIG. 3. Predictions for the ground-state energy of the planar rotor interacting with an external electric field, as given by different approximate methods. The solid line represents the variational method (exact results). The heavy dashed line represents second-order perturbation theory. The open triangles represent the Hartree method. The open circles represent the Monte Carlo calculation. The dotted line represents the Gaussian approximation. The dashed line represents the instantons calculation. The open squares represent the asymptotic expansions.

TABLE I. Ground-state energy for different values of λ obtained by the approximate methods developed in Secs. III–V. The values corresponding to the Matthieu approximation correspond to those obtained from the asymptotic expansion (3.2a) for $0.01 \leq \lambda < 0.4$ and from (3.3a) for $\lambda > 0.45$.

λ	$-E_0$ var.	$-E_0$ pert.	$-E_0$ Matt.	$-E_0$ Hartree	$-E_0$ Gaussian	$-E_0$ inst.
0.01	0.0001	0.0001	0.0001	· · ·	−0.0400	+0.0241
0.05	0.0024	0.0025	0.0025	· · ·	−0.0618	0.0798
0.10	0.0098	0.0100	0.0098	· · ·	−0.0581	0.0058
0.15	0.0216	0.0225	0.0217	· · ·	−0.0436	0.0054
0.20	0.0375	0.0400	0.0375	· · ·	−0.0236	0.0141
0.25	0.0569	0.0625	0.0568	· · ·	0.0000	0.0292
0.30	0.0792	0.0900	0.0786	· · ·	0.0261	0.0490
0.35	0.1039	0.1225	0.1037	· · ·	0.0542	0.0723
0.40	0.1307	0.1600	0.1221	· · ·	0.0838	0.0982
0.45	0.1593	0.2025	0.1496	0.1569	0.1146	0.1262
0.50	0.1892	0.2500	0.1812	0.1875	0.1464	0.1558
0.55	0.2204	0.3025	0.2137	0.2193	0.1792	0.1868
0.60	0.2526	0.3600	0.2471	0.2521	0.2127	0.2190
0.65	0.2858	0.4225	0.2811	0.2857	0.2469	0.2521
0.70	0.3197	0.4900	0.3158	0.3200	0.2817	0.2860
0.75	0.3543	0.5625	0.3510	0.3549	0.3170	0.3206
0.80	0.3895	0.6400	0.3867	0.3904	0.3528	0.3558
0.85	0.4252	0.7225	0.4228	0.4263	0.3890	0.3915
0.90	0.4614	0.8100	0.4594	0.4627	0.4257	0.4278
0.95	0.4980	0.9025	0.4963	0.4995	0.4627	0.4645
1.00	0.5350	1.0000	0.5336	0.5366	0.5000	0.5015
1.10	0.6101	1.2100	0.6090	0.6119	0.5756	0.6130
1.20	0.6864	1.4400	0.6856	0.6882	0.6523	0.6890
1.30	0.7638	1.6900	0.7631	0.7656	0.7299	0.7662
1.40	0.8420	1.9600	0.8416	0.8439	0.8084	0.8443
1.50	0.9211	2.2500	0.9207	0.9229	0.8876	0.9232
1.60	1.0009	2.5600	1.0006	1.0027	0.9675	1.0030
1.70	1.0813	2.8900	1.0810	1.0831	1.0481	1.0833
1.80	1.1623	3.2400	1.1621	1.1640	1.1292	1.1642
1.90	1.2438	3.6100	1.2437	1.2455	1.2108	1.2456
2.00	1.3258	4.0000	1.3257	1.3275	1.2929	1.3276

IV. SOME NUMERICAL METHODS

A. Variational method

Now we consider different methods in order to numerically approximate the eigenvalues of the planar rotor interacting with an external electric field,

$$H = -\frac{1}{2}\frac{d^2}{d\theta^2} + \lambda\cos\theta \,, \tag{4.1}$$

under the assumption of periodic boundary conditions.

The first technique under consideration is the well-known Tamm-Dancoff method.[12] Take N members of some arbitrary complete set of basic vectors. Here this set will be the eigenvectors of the "free problem"

$$H_0 = -\frac{1}{2}\frac{d^2}{d\theta^2} \,, \tag{4.2}$$

i.e.,

$$\psi_n = \frac{1}{\sqrt{2\pi}} e^{in\theta} \,. \tag{4.3}$$

One then constructs the $N \times N$ matrix representation of H:

$$H_{ij} = \int \psi_i^* H \psi_j d\theta, \; i,j = 1,2,\ldots,N$$

and one considers the corresponding eigenvalue equation

$$|H_{ij} - E\delta_{ij}| = 0, \quad i,j = 1,2,\ldots,N \,. \tag{4.4}$$

After getting the numerical solution of (4.4) for the eigenvalues, the question is "how rapidly does this sequence of approximate eigenvalues arrived at by systematically increasing the set (4.3) converge to the true eigenvalue?"

We organize the increasing-size Hamiltonian matrix following the "natural sequence"

$$0;+1,-1;+2,-2:+3,-3:\ldots;$$
$$\frac{(N-1)}{2},-\frac{(N-1)}{2}$$

for the index n in (4.3).

We have experimentally observed that ψ_n happens to be a very adequate basis to develop the eigenvectors of H. The rate of convergence is very high for practically any value of λ. Although we cannot prove any rigorous statement about the error we make, the numerical evidence is overwhelming to conclude that all the figures we collect in the tables are good digits for this problem. In fact, they are coincident with the exact results obtained above by using the asymptotic behavior ($\lambda\to\infty$) of Matthieu functions. This comparison of results is enough because due to our choice of the trial basis (4.3), this method will find more difficulties as the value of λ grows.

The value of a general matrix element H_{nm} is

$$H_{nm}=\frac{1}{2\pi}\int_0^{2\pi}e^{-in\theta}\left[-\frac{1}{2}\frac{d^2}{d\theta^2}+\lambda\cos\theta\right]e^{im\theta}d\theta$$
$$=\tfrac{1}{2}m^2\delta_{n,m}+\frac{\lambda}{2}(\delta_{n,m+1}+\delta_{n,m-1}), \quad (4.5)$$

which makes the task of putting the H_{nm} matrix in the computer a trivial one.

The results of this method are displayed in the second column of Table I for any value of the coupling constant λ. We would like to remark that the maximum size of the matrix we have used in the computations has been 17×17.

B. Perturbation theory

Should one consider

$$V=\lambda\cos\theta \quad (4.6)$$

as a perturbation potential of the free problem (4.2), the first correction to the unperturbed energy levels appears as a second-order effect, proportional to λ^2:

$$\Delta_2E_m=\lambda^2\frac{1}{4m^2-1}, \quad |m|\neq1 \quad (4.7)$$

which shows that the degeneracy is maintained up to this order. For the particular case $|m|=1$ the degeneracy is removed in second order. The results are

$$\Delta_2E_1=\tfrac{5}{6}\lambda^2, \quad \Delta_2E_{-1}=-\tfrac{1}{6}\lambda^2. \quad (4.8)$$

The perturbative numerical results appear in the third column of Table I. As expected their error increases as λ becomes large.

C. Approximation by a nonperiodic potential: Hartree method

Now, our first step is to expand the potential about its minimum $\theta=\pi$:

$$V=\lambda\left[-1+\tfrac{1}{2}(\pi-\theta)^2-\frac{1}{4!}(\pi-\theta)^4+\cdots\right], \quad \eta\equiv\pi-\theta. \quad (4.9)$$

If one keeps only the terms up to second order in η and forgets the periodic nature of the original problem, we obtain the approximate Hamiltonian

$$H_2=-\frac{1}{2}\frac{d^2}{d\eta^2}+\frac{\lambda}{2}\eta^2-\lambda, \quad -\infty<\eta<\infty \quad (4.10)$$

which provides the linear harmonic-oscillator spectrum

$$E_2(\eta)=\sqrt{\lambda}(n+\tfrac{1}{2})-\lambda, \quad (4.11)$$

in particular,

$$E_2(0)=-\lambda+\tfrac{1}{2}\sqrt{\lambda}. \quad (4.12)$$

From the functional point of view this approximation corresponds to performing a Gaussian integration about the classical solution $\bar{\theta}=\pi$.

In order to improve this Gaussian approximation we will keep, up to fourth order in η,

$$H_4=-\frac{1}{2}\frac{d^2}{d\eta^2}+\frac{\lambda}{2}\eta^2-\lambda-\frac{\lambda}{24}\eta^4. \quad (4.13)$$

The bold consideration of η as a nonangular variable in H_4 is obviously meaningless, therefore we now proceed to linearize H_4 in order to (i) convert H_4 in a sensible problem and (ii) maintain some of the nonlinear information buried in H_4. We specifically follow the method used by Chang for the anharmonic oscillator[13] which consists in the replacement

$$\eta^4\to6\langle\eta^2\rangle\eta^2-3\langle\eta^2\rangle^2. \quad (4.14)$$

This is a Hartree-type approximation, because we keep only the lowest-order quantum fluctuations. Under this approximation

$$H_4\to H_4'=-\frac{1}{2}\frac{d^2}{d\eta^2}+\lambda\left[-1+\frac{1}{2}\left[1-\frac{\langle\eta^2\rangle}{2}\right]\eta^2+\tfrac{1}{8}\langle\eta^2\rangle^2\right],$$
$$K\equiv1-\frac{\langle\eta^2\rangle}{2}. \quad (4.15)$$

Hence, whenever $K>0$ we may assume that η is a noncompact variable whose range varies from $-\infty$ to $+\infty$. From (4.15) we can compute the expectation value of η^2. Using the virial theorem for the ground state we get

$$\langle\eta^2\rangle=\frac{1}{\sqrt{K}}\ . \tag{4.16}$$

To fix $\langle\eta^2\rangle$ we impose the self-consistency requirement that the $\langle\eta^2\rangle$ introduced in the frequency K is the same as obtained in (4.16). $\langle\eta^2\rangle$ obeys a cubic equation

$$\begin{aligned}&2\lambda x^3-4\lambda x^2+1=0\ ,\\ &x\equiv\langle\eta^2\rangle\ .\end{aligned} \tag{4.17}$$

The solution of (4.17) in the limit of large λ provides the following result:

$$E_4(0)\underset{\lambda\to\infty}{\sim}\tfrac{1}{2}\sqrt{\lambda}-\lambda-\tfrac{1}{32}\ , \tag{4.18}$$

which is coincident with the exact asymptotic behavior.

In general the prediction of the method for the ground state is

$$E_4(0)=-\lambda+\tfrac{1}{2}\sqrt{K\lambda}+\tfrac{1}{8}\lambda\langle\eta^2\rangle^2 \tag{4.19}$$

and there exists a minimum of λ ($\lambda_{\min}$), so that for $\lambda<\lambda_{\min}$, $K<0$ and the whole scheme breaks down.

The numerical results from the method are collected in the fifth column of Table I.

V. INSTANTON APPROXIMATION

Next we are going to estimate the ground-state energy of the interacting system by functional path-integral methods.[14] The starting point is the quantum Euclidean propagator

$$\begin{aligned}K_E(T,\pi,\{\pi\})&=\langle\{\pi\}\,|\,e^{-HT}\,|\,\pi\rangle\\ &=\sum_{n=-\infty}^{+\infty}e^{-E_nT}\varphi_n^*(\{\pi\})\varphi_n(\pi)\ ,\end{aligned} \tag{5.1}$$

where

$$H_\lambda\varphi_n(\theta)=E_n\varphi_n(\theta)\ .$$

When $T\to\infty$, the T behavior of (5.2) is dominated by the ground-state contribution e^{-E_0T}. The path-integral representation of the propagator is

$$K_E(T;\pi,\{\pi\})=N\int_{\theta(-T/2)=\pi}^{\{\theta(T/2)\}=\{\pi\}}\prod_t d\theta(t)e^{S_E[\theta(t)]}\ , \tag{5.2}$$

where

$$S_E[\theta(t)]=-\int_{-T/2}^{T/2}dt\left(\tfrac{1}{2}\dot\theta^2+\lambda\cos\theta\right) \tag{5.3}$$

is the Euclidean action. Hereafter in this section we shall consider the potential term $V(\theta)=\lambda\cos\theta$ moved to $\bar V(\theta)=\lambda[1+\cos(\theta)]$ in order to deal with positive energy; thus the energy levels $\bar E_n$ become modified in an amount of λ ($E_n=\bar E_n-\lambda$).

In the semiclassical limit, the path integral (5.2) is dominated by the contribution of paths lying around stationary paths of $\bar S_E=S_E-\lambda T$ verifying the boundary conditions

$$\theta\left[-\frac{T}{2}\right]=\pi,\quad\left\{\theta\left[+\frac{T}{2}\right]\right\}=\{\pi\} \tag{5.4}$$

when $T\to\infty$. Such stationary paths $\bar\theta(t)$ are the solutions of the differential equation

$$\frac{\delta\bar S_E(\theta)}{\delta\theta}=0=-\frac{1}{2}\frac{d^2\bar\theta(t)}{dt^2}-\lambda\sin(\bar\theta(t))\ . \tag{5.5}$$

Notice that (5.5) is the classical equation of motion of the particle in an effective potential $-\bar V(\theta)$ [see Figs. 4(a) and 4(b)]. Equation (5.5) coincides also with the spatial sine-Gordon equation for static scalar fields. Therefore, there are three solutions of (5.5) with the boundary conditions (4.4):

$$\bar\theta_0(t)=\pi\ \text{(static)}\ , \tag{5.6}$$

$$\bar\theta_1(t)=-\pi+4\arctan\{\exp[\sqrt{\lambda}(t-t_0)]\}\ \text{(instanton)}, \tag{5.7}$$

$$\bar\theta_{-1}(t)=-3\pi+4\arctan\{\exp[-\sqrt{\lambda}(t-t_0)]\}$$

$$\text{(anti-instanton)}\ , \tag{5.8}$$

where t_0 is an arbitrary time parameter with $\{\bar\theta(t_0)\}=\{0\}$ (Ref. 15) [see Figs. 5(a) and 5(b)]. The instanton and anti-instanton solutions only verify

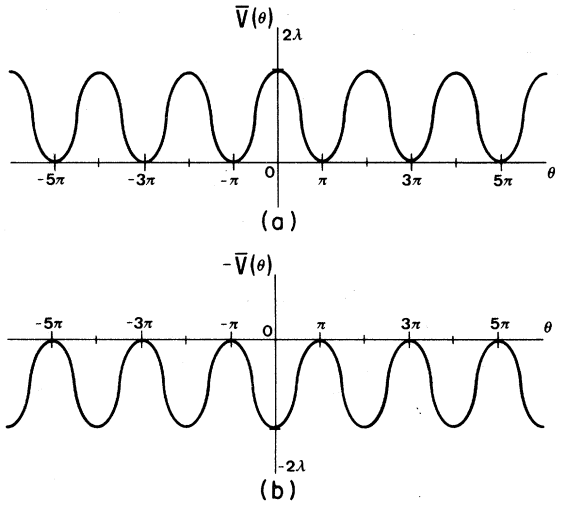

FIG. 4. (a) Electric potential. (b) Euclidean potential.

the boundary conditions (5.4) when $T\to\infty$ and correspond to the soliton and antisoliton of the sine-Gordon equation.

The contribution to (5.2) of the paths around a stationary path $\bar{\theta}(t)$ can be estimated expanding the paths in a neighborhood of $\bar{\theta}(t)$ in terms of the eigenfunctions $\theta_n(t)$ of the differential operator

$$-\frac{d^2}{dt^2}+\frac{d^2\bar{V}(\theta)}{d\theta^2}$$

vanishing at the boundaries $+T/2$ and $-T/2$:

$$\theta(t)=\bar{\theta}(t)+\sum_n a_n\theta_n(t) \tag{5.9}$$

by using that expression in (5.2) and retaining only terms up to second order in powers of θ_n (which corresponds to considering only lowest terms on $\hbar$), we obtain the result that the contribution to $K_E(T;\pi,\{\pi\})$ due to the paths in a neighborhood of $\bar{\theta}(t)$ is given by

$$N\exp[\bar{S}_E(\bar{\theta})]\{\det[-d_t^2-\lambda\cos(\bar{\theta}(t))]\}^{-1/2}\,. \tag{5.10}$$

In the case of the static stationary solution (5.6), this approximation is equivalent to considering the Taylor expansion of $\bar{V}$ up to second order around its minimum at $\theta=\pi$.

In order to eliminate the divergences in (5.10), the determinant of $-[\partial_t^2+\lambda\cos\bar{\theta}(t)]$ has to be considered in a renormalized way, i.e., the zero mode contribution has to be computed by collective-coordinate methods as we shall see further.

Since we consider terms only up to second order we are carrying out a Gaussian integration around the stationary configurations. Thus, we are in fact integrating only over a neighborhood of each stationary configuration, and then we have to add separately the contribution of paths around each stationary configuration.

The contribution to $K_E(T;\pi,\{\pi\})$ arising from paths around $\bar{\theta}_0(t)=\pi$, K_E^0, is given by (5.10) taking into account that[2]

$$N[\det(-d_t^2+\lambda)]^{-1/2}=[\pi\psi_0(T/2)]^{-1/2}\,, \tag{5.11}$$

where ψ_0 is the solution of the equation

$$(-d_t^2+\lambda)\psi_0=0 \tag{5.12}$$

determined by the Cauchy conditions

$$\psi_0=\left[-\frac{T}{2}\right]=0,\quad \partial_t\psi_0\left[-\frac{T}{2}\right]=1\,.$$

Thus

$$K_E^0=\lambda^{1/4}\pi^{-1/2}\exp\left[-\lambda^{1/2}\frac{T}{2}\right]. \tag{5.13}$$

The contribution to the Euclidean propagator arising from the instanton sector K_E^1 is given by[2]

$$K_E^1=K_E^0KT\exp(-\bar{S}_E^1) \tag{5.14}$$

when

$$K=\left[\frac{\bar{S}_E^1}{2\pi}\right]^{1/2}D^{1/2}\,, \tag{5.15}$$

$$\bar{S}_E^1=\int_{-\pi}^{+\pi}d\theta\sqrt{2V(\theta)}=8\sqrt{\lambda}\,, \tag{5.16}$$

$$D=\left|\frac{\det(-d_t^2+\lambda)}{\det'[-d_t^2-\cos(\bar{\theta}_1(t))]}\right|^{1/2} \tag{5.17}$$

with $\det'[-d_t^2-\cos(\bar{\theta}_1(t))]$ being the renormalized determinant of the differential operator $[-d_t^2-\cos(\bar{\theta}_1(t))]$, i.e., without contribution of zero modes. The zero modes have been taken into account simply by integrating in the collective coordinate (center of the instanton) which gives a contribution of the factor T in (5.14).

The estimation of D can be done taking into account that $D=2A^2\sqrt{\lambda}$, where A is the coefficient which governs the behavior of

$$\theta_*=(\bar{S}_E^1)^{-1/2}\frac{d\bar{\theta}}{dt} \tag{5.18}$$

when t goes to $\pm\infty$, i.e.,

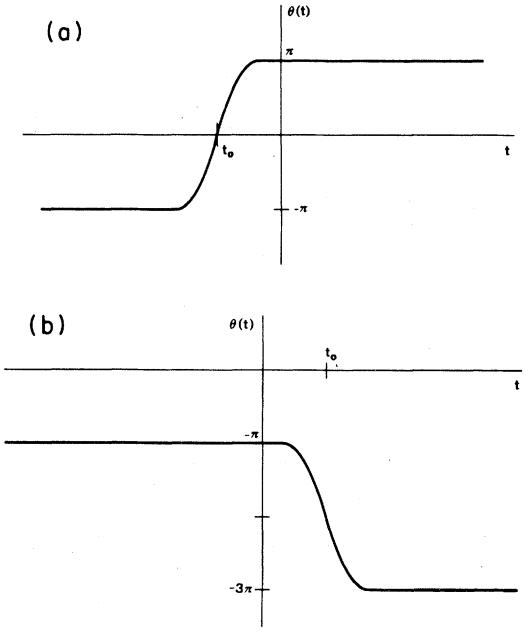

FIG. 5. (a) Instanton, (b) anti-instanton.

$$\theta_*(t)\to Ae^{-|t|\sqrt{\lambda}},\quad t\to\pm\infty\ .$$

Using (5.7) and (5.18) we obtain $A=\sqrt{2}\lambda^{1/4}$. Thus,

$$K=4\pi^{-1/2}\lambda^{3/4}\ . \tag{5.19}$$

It is easy to show that the anti-instanton contribution is the same as that of the instanton. As is well known the contributions arising from paths around configurations with n instantons and $\bar{n}$ anti-instantons are also relevant in spite of the fact that such configurations are only approximate solutions of the Euclidean equation (5.5).

The Gaussian integration over the paths in a neighborhood of a configuration with n instantons and $\bar{n}$ anti-instantons can be evaluated in the dilute-gas approximation. This approximation consists in assuming that the highest contribution arises from the configurations where the instantons and anti-instantons are widely separated [see Figs. 6(a) and 6(b)]. Such a contribution is given by

$$K_E^{n,\bar{n}}=K_E^0K^{n+\bar{n}}T^{n+\bar{n}}[(n+\bar{n})!]^{-1}\times\exp[-(n+\bar{n})\exp(-8\sqrt{\lambda})]\ , \tag{5.20}$$

where the factor $T^{n+\bar{n}}/(n+\bar{n})$ comes from the integration over the collective coordinates $(t_1^0\cdots t_n^0,t_1^0\cdots t_{\bar{n}}^0)$ of the centers of the instantons and anti-instantons.

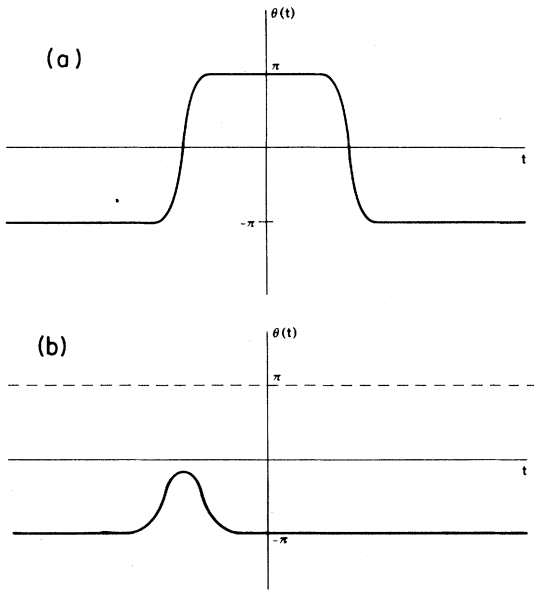

FIG. 6. Instanton—anti-instanton interactions: (a) dilute-gas regime, (b) dense-gas regime.

Since for any pair $(n,\bar{n})$ there always exist $\binom{n+\bar{n}}{n}$ configurations with n instantons and $\bar{n}$ anti-instantons satisfying the boundary conditions (5.4) the global contribution of stationary points to the propagator is given by

$$K_E=\sum_{n,\bar{n}=0}^{\infty}K_E^0K^{n+\bar{n}}T^{n+\bar{n}}(n!\bar{n}!)^{-1}\exp[-(n+\bar{n})\exp(-8\sqrt{\lambda})]=K_E^0\exp[2KT\exp(-8\sqrt{\lambda})]\ . \tag{5.21}$$

Now, according to (5.1), in the limit $T\to\infty$

$$K_E\approx e^{-(E_0+\lambda)T}\ . \tag{5.22}$$

Thus, by comparing (4.18) and (4.19) the ground-state energy of the system is given by

$$E_0=-\lambda+\tfrac{1}{2}\lambda^{1/2}-8\pi^{-1/2}\lambda^{3/4}\exp(-8\sqrt{\lambda})\ . \tag{5.23}$$

The comparison of this value with the exact one is displayed in Table I and Fig. 3. The expression (5.23) fits in a qualitative way rather well the λ behavior of the energy E_0 from $\lambda=0.1$ on. However, it can be shown that there is an asymptotic discrepancy of an amount $\frac{1}{32}$ with respect to the exact results. This discrepancy can be corrected by modifying the shape of the Gaussian approximation (see Sec. IV C).

The last term on the right-hand side of (5.23) gives the contribution to the ground-state energy due to the tunneling effect carried out by multi-instantons. It is noteworthy to observe as this term vanishes as λ increases to infinity which corresponds to the fact that tunneling effects disappear if the barrier of potential V [Figs. 4(a) and (b)] becomes infinite. Moreover, (5.23) shows that multi-instanton tunneling effects vanish much sooner than the Gaussian ones. On the other hand, in Fig. 3 it is pointed out that the discrepancy between exact values of E_0 and those provided by (5.23) increase as λ goes to zero. This fact is motivated by the falloff of the dilute-gas multi-instanton approximation for the small-λ region, as we will see in the next section.

VI. MONTE CARLO APPROXIMATION

This section is devoted to the computation of vacuum expectation values by means of the Monte Carlo technique, which was originally devised by Metropolis *et al.*[17] Our departing point is the vacuum expectation value of an operator A, i.e., the expectation value of such an operator in the ground

state of the system:

$$A_0=\langle 0|A|0\rangle = \lim_{T\to\infty}\frac{\int\prod_t d\theta(t)A(\theta(t))e^{S_E(\theta,T)}}{\int\prod_t d\theta(t)e^{S_E(\theta,T)}}. \tag{6.1}$$

In order to compute the integrals of (6.1) we will use the Feynman prescription,[16] i.e., we will divide the time coordinate in a fine lattice, using the following notation:

$$\theta(t_i)=\theta_i\ ,\quad t_{i+1}-t_i=a\ ,\quad T=Na\ , \tag{6.2}$$

where N is the total number of sites of the lattice. In such a case, the Euclidean action $S_E(\theta,T)$ will be given by

$$S_E(\theta,T)=-\sum_{j=1}^{N} a\left[\left[\frac{\theta_{j+1}-\theta_j}{a}\right]^2+V(\theta_j)\right]$$

and the ground-state energy will be

$$E_0=\lim_{N\to\infty}\frac{\int\prod_{i=1}^{N}d\theta_i H(\theta_1,\ldots,\theta_N)\exp\left\{-\sum_{j=1}^{N}a\left[\left[\frac{\theta_{j+1}-\theta_j}{a}\right]^2+V(\theta_j)\right]\right\}}{\int\prod_{i=1}^{N}d\theta_i\exp\left\{-\sum_{j=1}^{N}a\left[\left[\frac{\theta_{j+1}-\theta_j}{a}\right]^2+V(\theta_j)\right]\right\}}. \tag{6.3}$$

The computation of E_0 involves the evaluation of $2N$ integrals ($N\to\infty$) which constitutes an impossible task except in some special cases; therefore, the possibility of carrying out the sum by means of numerical generation of the trajectories is quite important. Denoting one of those trajectories by

$$\vec{\theta}^{\,\alpha}=(\theta_1^\alpha,\theta_2^\alpha,\ldots,\theta_n^\alpha)\ ,$$

then

$$E_0=\frac{\sum_\alpha H(\vec{\theta}^{\,\alpha})e^{S_E(\vec{\theta}^{\,\alpha})}}{\sum_\alpha e^{S_E(\vec{\theta}^{\,\alpha})}}\ , \tag{6.4}$$

where the sum on α is extended over all possible trajectories (paths). However, the evaluation of the contributions of the infinite trajectories to E_0 is again practically impossible, and all we can do is to approximate (6.4) by a sum over a finite number of relevant trajectories. If we choose trajectories $\vec{\theta}^{\,\beta}$ according to the Boltzmann distribution

$$P(\vec{\theta}^{\,\beta})=\frac{e^{S_E(\vec{\theta}^{\,\beta})}}{\sum_\alpha e^{S_E(\vec{\theta}^{\,\alpha})}}\ , \tag{6.5}$$

the expectation value for E_0 is

$$E_0=\frac{1}{M}\sum_{\alpha=1}^{M}E_0(\vec{\theta}^{\,\alpha})\ , \tag{6.6}$$

with M being the total number of trajectories used in the average and $E_0(\vec{\theta}^{\,\alpha})$ the energy of path $\vec{\theta}^{\,\alpha}$.

Now, the problem is how to find the M important paths $\vec{\theta}^{\,\beta}$ chosen according to the statistical weight (6.5). This is done by using a Markov process constructed, with the Metropolis criterion, in such a way that in the limit of $M\to\infty$ the probability of occurrence of the trajectory $\vec{\theta}^{\,\beta}$ is given by (6.5). In general the contributions to the sum are modulated by two facts, the first is the value of the Euclidean action associated with one trajectory because of (6.5) and the second is the number of trajectories whose action is identical. Basically the Metropolis method begins by choosing an initial trajectory $\vec{\theta}^{\,0}$ from which one generates quite at random a new trajecotry $\vec{\theta}\,'$ and computes

$$\Delta S=S_E(\vec{\theta}\,')-S_E(\vec{\theta}^{\,0}) \tag{6.7}$$

if $\Delta S>0$, $\vec{\theta}^{\,0}$ is substituted by $\vec{\theta}\,'$ (i.e., the appearance of trajectories with small Euclidean action is favored); on the contrary, if $\Delta S\leq 0$, a number r generated at random between 0 and 1 is compared with $e^{\Delta S}$, if $r<e^{\Delta S}$, $\vec{\theta}^{\,0}$ is substituted by $\vec{\theta}\,'$ and if $r>e^{\Delta S}$, $\vec{\theta}\,'$ is left out and the computer maintains $\vec{\theta}^{\,0}$.

This process is iterated q times (q should be large enough) until an equilibrium trajectory is reached

[i.e., a trajectory of maximum contribution to (6.3)]. This equilibrium trajectory is used to do a measurement of the energy. The set of steps quoted above, in which one begins in $\vec{\theta}^0$ and ends in equilibrium trajectory, will be called "to have completed a cycle." After M cycles, E_0 will be given by (6.6).

However, as the crucial question with the Monte Carlo method lies on the time, consumed by the computer on each cycle, it is necessary to do some technical precisions in order to make this technique truly efficient.

When one computes the ground-state energy, one should remember[16] that only the nondifferentiable trajectories contribute to (6.3), and therefore it is not possible to define a mean quadratic velocity in a point because

$$\left\langle \left[\frac{\theta_{i+1}-\theta_i}{a} \right]^2 \right\rangle = \frac{1}{a} + O(1), \quad a \to 0 . \tag{6.8}$$

Therefore, in order to compute the mean kinetic energy we shall define the mean quadratic velocity after Feynman and Hibbs as

$$\langle v_i^2 \rangle = - \frac{\langle (\theta_{i+1}-\theta_i)(\theta_i-\theta_{i-1}) \rangle}{a^2} \tag{6.9}$$

or we can make use of the virial theorem to compute the expectation value of the kinetic energy T:

$$\langle T \rangle = \frac{1}{2} \left\langle \theta \frac{dV(\theta)}{d\theta} \right\rangle . \tag{6.10}$$

In order to shorten the distance between the initial and the equilibrium trajectories it is important to choose $\vec{\theta}^0$ close enough to the latter one. It calls for previous information about the solution. A practical hint in the situations where the semiclassical ansatz is a good approximation consists in taking $\vec{\theta}^0$ as the solution of the classical equations of motion. On the other hand, it is important to bear in mind that when a new trajectory is generated from a previous one, the Euclidean action associated with them should not differ too much, because otherwise the criterion of Metropolis will usually reject it. Therefore, it is convenient to generate a new trajectory by moving only one coordinate ($\theta_i \to \theta_i'$) at one time; furthermore, although in principle θ_i may vary between $(-\infty, +\infty)$, it is convenient that the new generated coordinate will not differ too much from the previous one. Therefore, it is usual to introduce a parameter Δ, so that the new value fulfills

$$\theta_i - \Delta \le \theta_i' \le \theta_i + \Delta . \tag{6.11}$$

One should also recall that before completing a cycle we should allow all the coordinates the chance of moving themselves sufficiently so as to attain an equilibrium trajectory; therefore, we will move each coordinate a number of times S, and we will try to fulfill the following rule: $S\Delta$ should be bigger than a typical distance between two equilibrium trajectories of our problem (in the case of the rotor, we have used $S\Delta > 4\pi$). In our lattice, in order to minimize border effects we have used periodic boundary conditions ($\{\theta_1\} = \{\theta_N\}$); thus in the process of completing a cycle we will begin with a trajectory $\vec{\theta}_0$ and we will move θ_1^0 S times, applying the Metropolis criterion at every time, then we will do the same with θ_2^0, and so on until θ_N^0, and at this moment the first cycle will be completed. On each cycle the beginning trajectory will be the equilibrium trajectory of the previous cycle, but in order to assure ourselves that there is no correlation between the equilibrium trajectories used to do the measurements and that the result is independent of the initial trajectory we chose in the first cycle, we will maintain the method by carrying out a number $\bar{N}$ of initial cycles (typically $\bar{N} = 10,20$) without measuring anything, and from $\bar{N}$ on between two consecutive measurements, we will complete three cycles without measuring anything either.

In our program the parameters were chosen as follows: The time lattice spacing, which should be less than the characteristic period of our problem T_0, is generally

$$\frac{a}{T_0} \in [\tfrac{1}{20}, \tfrac{1}{30}] \tag{6.12}$$

with

$$T_0 = \frac{2\pi}{E_0} \hbar . \tag{6.13}$$

Furthermore, $N = 1000$, hence Na is big enough so as to pick only the ground-state contribution. With respect to S (number of times a coordinate θ_1 is moved on each cycle), it was taken typically between 10 and 15 interactions. As $V = \Delta/a$ is the maximum velocity one allows on each change of the coordinates, we have taken V bigger than the typical velocity of the problem $V_0 = \sqrt{2E_0}$, specifically $V/V_0 \simeq 2$, 3, or 4, which leads to

$$\Delta = K\sqrt{a}, \quad K \simeq [2,4] . \tag{6.14}$$

The ground-state energy E_0 has been computed by averaging M times the energy of different equilibrium configurations ($M = 100$). The statistical fluctuations of the energy on each average is given by

$$\Delta E_0 = \frac{[(\Delta E_0)^2]^{1/2}}{|E_0|} \simeq \frac{1}{\sqrt{N}} .$$

In Table II we present our results.[18] There one may check that although the Monte Carlo method is not terribly precise, their results are in good agreement

with the exact results and it is especially useful to study the qualitative features of the problem. In particular in Figs. 7(a)–7(c), three typical equilibrium trajectories have been plotted. In Fig. 7(a), for $\lambda=0.01$, where the dilute-gas approximation in the instanton method starts becoming incorrect, one may observe a typical configuration of interacting multi-instantons. In Fig. 7(b), for $\lambda=0.2$ a typical equilibrium trajectory already presents configurations with well-separated instantons. Finally, for $\lambda=2$ the effects of instantons have disappeared and the dominant trajectories are those with small fluctuations around the classical one $\bar{\theta}=\pi$.

VII. ϵ VACUUM

Let us now consider the general situation where the rotor is acted upon by the action of the electric field while a non-null magnetic flux $2\pi\epsilon$ flows across the rotor circle, which simulates the ϵ-vacuum situation of the original system.

The classical Lagrangian in this case is given by

$$L_E=\tfrac{1}{2}(\dot{\theta}-\epsilon)^2-\tfrac{1}{2}\epsilon^2-\lambda\cos\theta \tag{7.1}$$

and the corresponding quantum Hamiltonian is

$$H_\epsilon=-\frac{1}{2}\left[\frac{d}{d\theta}-i\epsilon\right]^2+\lambda\cos\theta\ . \tag{7.2}$$

The path-integral representation of the propagator

TABLE II. Ground-state energy for different values of the electric field strength λ calculated by the Monte Carlo method for fixed values of the space (Δ) and temporal (a) lattice intervals.

λ	$-E_0$	Δ	a
0.1	0.005	2	1
0.2	0.031	1.42	0.51
0.3	0.068	2	1
0.4	0.126	2	1
0.5	0.19	2	1
0.6	0.257	2	1
0.7	0.312	1.4	0.5
0.8	0.394	1.6	0.7
0.9	0.463	1.6	0.7
1	0.546	1.6	0.6
1.1	0.621	1.6	0.6
1.2	0.695	1.6	0.6
1.3	0.773	1.4	0.5
1.4	0.866	1.6	0.7
1.5	0.924	1.4	0.33
1.6	0.978	1.4	0.33
1.7	1.075	1.2	0.33
1.8	1.165	1.2	0.33
1.9	1.254	1.4	0.33
2	1.33	1.4	0.33

is given by

$$K_E^\epsilon(T,\pi\{\pi\})=N\int_{\theta(-T/2)=\pi}^{\{\theta(T/2)\}=\{\pi\}}\prod_t d\theta(t)e^{S_E^\epsilon(\theta,t)}\ , \tag{7.3}$$

where

$$S_E^\epsilon(\theta,T)=-\int_{-T/2}^{+T/2}dt(\tfrac{1}{2}\dot{\theta}^2+\lambda\cos\theta+i\epsilon\dot{\theta})\ . \tag{7.4}$$

In the same way as in the free case the additional dependent term contributes giving rise to a weight factor $e^{-i2\pi\epsilon\chi[\theta(t)]}$ for each path sector depending only on the winding number of $\theta(t)$. This interference term is the physical response of the system to the magnetic field.

Therefore, if we estimate the propagator by using the dilute-gas multi-instanton approximation in this case we obtain

$$K_E^\epsilon=\sum_{n,\bar{n}=0}^{\infty}K_E^0K^{n+\bar{n}}T^{n+\bar{n}}\frac{1}{n!\bar{n}!}\times\exp[(n+\bar{n})e^{-8\sqrt{\lambda}}-i2\pi\epsilon(n-\bar{n})] \tag{7.5}$$

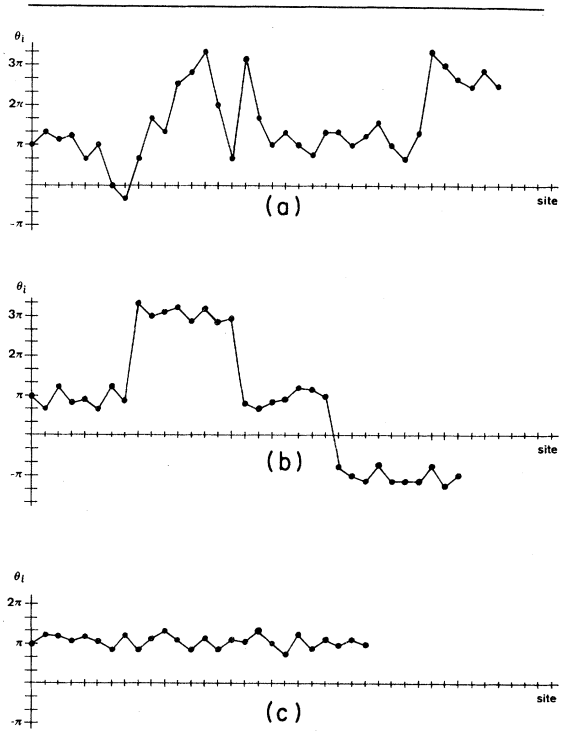

FIG. 7. Typical equilibrium trajectories in the Monte Carlo method. (a) $\lambda=0.01$. Here the dilute-gas approximation breaks down. (b) $\lambda=0.2$. Dilute-gas regime. (c) $\lambda=0.2$. Classical regime with small fluctuations about $\theta=\pi$.

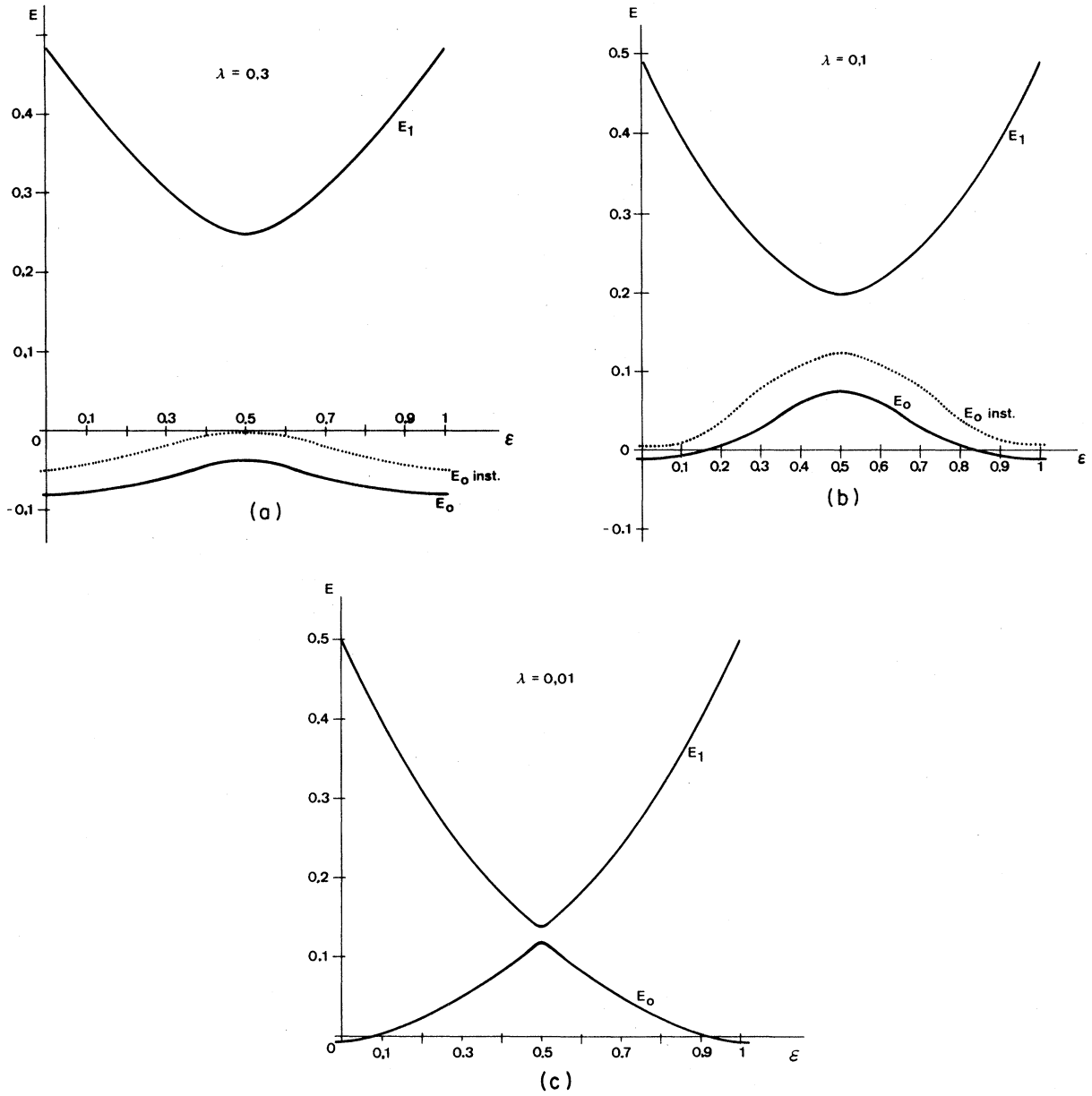

FIG. 8. Graphical representation of the two lowest energy levels of the rotor, for different values of λ and ϵ. The solid line represents variational results and the dashed line represents the instantons (dilute-gas) calculation.

because the winding number of the multi-instanton $(n,\bar{n})$ configuration is $n-\bar{n}$.

Thus the ground-state energy in this approximation is given by

$$E_0^{\epsilon}=-\lambda+\tfrac{1}{2}\lambda^{1/2}-8\pi^{1/2}\lambda^{3/4}e^{-8\sqrt{\lambda}}\cos(2\pi\epsilon)\ . \tag{7.6}$$

Of course, this value reduces to (4.20) when $\epsilon=0$. In the case $\epsilon=\frac{1}{2}$ the third term in (7.6) becomes positive, which implies that the corresponding magnetic flux generates a destructive interference between instantons. This prediction of the dilute-gas instanton approximation is verified in practice by using the variational techniques developed in Sec. IV A [Figs. 9(a)–9(c)]. In fact, for $\epsilon=\frac{1}{2}$ the ground-state wave function vanishes at $\theta=0$ for any λ, which represents the minimal tunneling situation. However, the degeneracy existing for $\lambda=0$ is broken for any $\lambda>0$ [see Tables III, IV and Figs. 8(a)–8(c)] the ϵ dependence of the ground-state energy becomes regular (disappearance of the "phase transi-

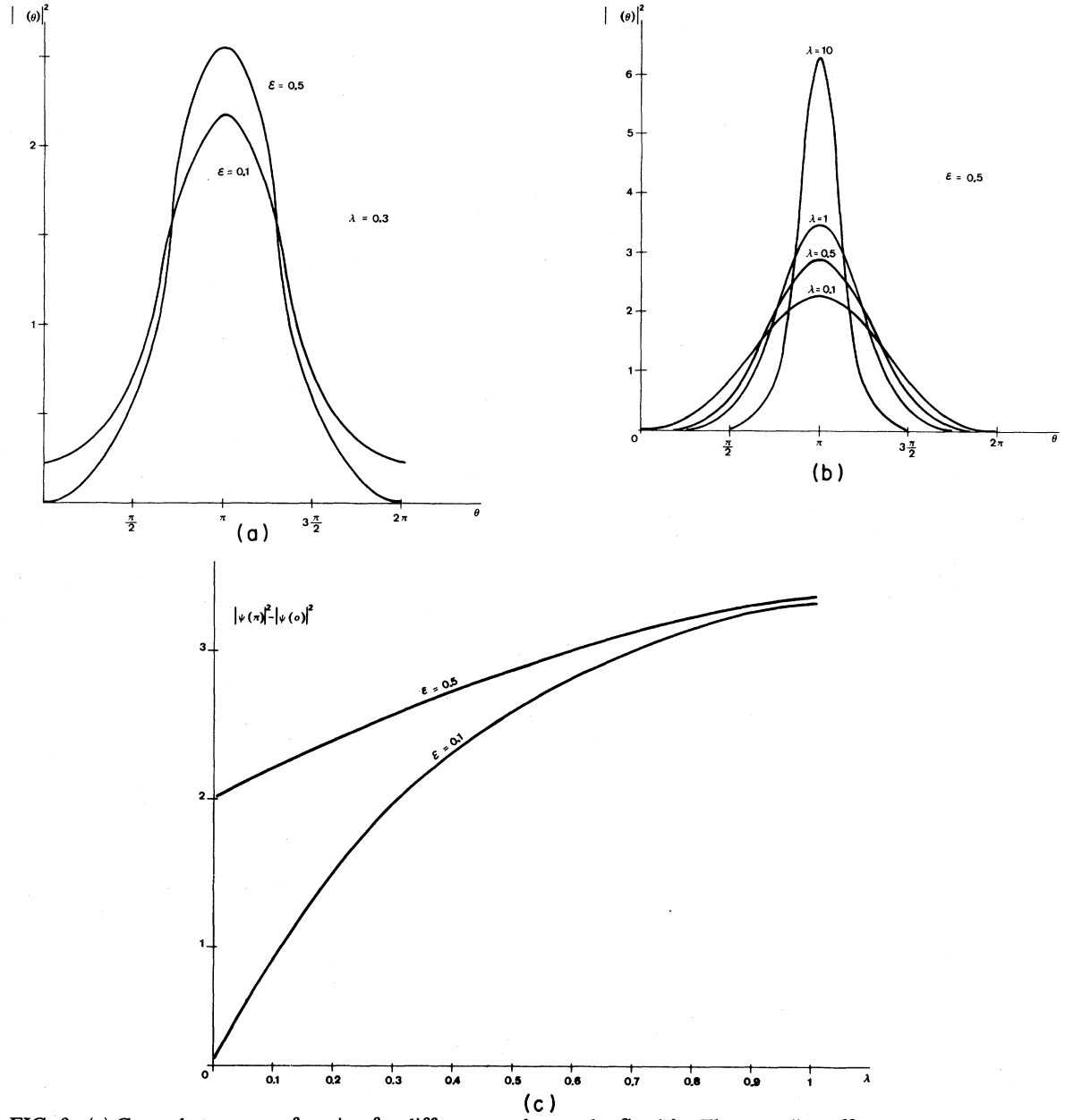

FIG. 9. (a) Ground-state wave function for different ϵ values and a fixed λ. The tunneling effect weakens as ϵ becomes 0.5. (b) Ground-state wave function for $\epsilon=0.5$ and different values of λ. The tunneling effect weakens as λ increases but the wave function is always 0 in $\theta=0$, for any λ. (c) Plot of $|\psi(\pi)|^2-|\psi(0)|^2$ as a function of λ, for two different values of ϵ.

tion"). This regularity can be analytically proved as a consequence of the nondegeneracy of the ground state and the analytic dependence of H_ϵ on ϵ.[19] This breaking of the degeneracy at $\epsilon=\frac{1}{2}$ increases as λ grows [see Figs. 8(a)–8(c)]. As expected, tunneling effects are diminished as λ increases to infinity [Figs. 9(b) and 9(c)].

Finally, the prediction for the ground-state energy obtained from perturbation theory is given by

$$E_0^\epsilon=\begin{cases}\frac{1}{2}\epsilon^2+\dfrac{\lambda^2}{4\epsilon^2+1}, & 0\le\epsilon\le\frac{1}{2}\\ \frac{1}{2}(1-\epsilon)^2+\dfrac{\lambda^2}{4(1-\epsilon)^2-1}, & \frac{1}{2}\ll\epsilon\le 1,\end{cases} \tag{7.7}$$

TABLE III. ϵ-vacuum energy for different values of the electric field strength λ.

ϵ \ λ	0.01	0.1	0.3
0	−0.0001	−0.0098	−0.0792
0.1	0.0049	−0.0052	−0.0764
0.2	0.0199	0.0084	−0.0688
0.3	0.0448	0.0294	−0.0582
0.4	0.0797	0.0567	−0.0485
0.5	0.1200	0.0726	−0.0444
0.6	0.0797	0.0567	−0.0485
0.7	0.0448	0.0294	−0.0582
0.8	0.0199	0.0084	−0.0688
0.9	0.0049	−0.0052	−0.0764
1	−0.0001	−0.0098	−0.0792

TABLE IV. Energy of the lowest excited state of different ϵ realizations and different values of λ.

ϵ \ λ	0.01	0.1	0.3
0	0.5000	0.4983	0.4895
0.1	0.4050	0.4092	0.4287
0.2	0.3201	0.3261	0.3580
0.3	0.2451	0.2567	0.3008
0.4	0.1802	0.1983	0.2627
0.5	0.1300	0.1724	0.2491
0.6	0.1802	0.1983	0.2627
0.7	0.2451	0.2567	0.3008
0.8	0.3201	0.3261	0.3580
0.9	0.4050	0.4092	0.4287
1	0.5000	0.4983	0.4895

$$E_0^{\epsilon}=\begin{cases}\frac{1}{2}\epsilon^2-\frac{\lambda}{2}, & 0\ll\epsilon\leq\frac{1}{2}\\ \frac{1}{2}(1-\epsilon)^2-\frac{\lambda}{2}, & \frac{1}{2}\leq\epsilon\ll 1\end{cases} \tag{7.8}$$

which fits rather well the exact results for $\lambda<0.3$. However, for large λ, the nonperturbative predictions (7.6) is more suitable.

VIII. CONCLUSIONS

From the numerical results obtained by applying the different approximate methods, we may draw several conclusions. First one should remark that the best numerical results are provided, for any values of λ and ϵ, by the variational method. In fact, we will consider these numbers as the exact results of the problem.

For $\epsilon=0$, second-order perturbation theory provides, as expected, accurate results (better than 4%) for a coupling strength lower than $\lambda<0.5$.

The instanton method applied in Sec. V starts fitting the qualitative features of the exact result for $\lambda>0.01$ (the quantitative agreement is about 50%) and for $\lambda>0.8$ (the numerical agreement is already very good) the instanton contribution comes essentially from the Gaussian approximation performed about the static classical solution $\theta=\pi$. One understands this phenomenon by remembering the range of validity of the dilute-gas instanton method. The numerical results show that for $\lambda<0.1$ the gas of multi-instantons becomes dense (as depicted in Fig. 7, this phenomenon may be observed "physically" in the Monte Carlo simulation); from $0.1<\lambda<0.8$ the contribution of the dilute gas is important, whereas for $\lambda>0.8$, the Gaussian approximation makes the instanton contribution negligible (the gas is evaporated). Although for $\lambda>0.8$ the numerical agreement is increasingly good, there always remains a difference of $\frac{1}{32}$ as an asymptotic discrepancy with the exact result.

This asymptotic difference is corrected in an exact way when one performs an effective Gaussian approximation in the Hartree-type method, as explained in Sec. IV. This method provides extremely accurate results for any value of λ varying within the range where the method is applicable ($\lambda>0.4$).

The Monte Carlo method describes qualitatively well the energy of the ground state for any λ. It also shows pictorially the qualitative changes (depending on λ) in the density of instanton configurations: diluted, dense, etc. (see Fig. 7). From the numerical point of view, should one choose adequately the increments of the effective lattice, this method may be more precise than the instanton technique, even for a very large value of λ. Nevertheless, it cannot compete at all with the variational one.

The physics of the model changes strikingly when one "connects" the ϵ vacuum. In the free case ($\lambda=0$), for $\epsilon=\frac{1}{2}$, the ground state becomes degenerate, and consequently there appears a discontinuity in the first derivative of its energy with respect to ϵ in that point ("phase transition"). When the interaction is switched on, that degeneracy disappears for any value of λ, and in the position $\epsilon=\frac{1}{2}$ the gap between the first two levels grows monotonically with λ. This phenomenon is connected, as the instanton calculation shows, to the fact that for $\epsilon=\frac{1}{2}$, the biggest destructive interference between instantons happens, which provokes the diminution of the tunnel effect. This fact may be checked more precisely by looking at the results of the variational calculation; it shows that the position probability density vanishes exactly at $\theta=0$ for the case $\epsilon=\frac{1}{2}$ and any nonzero value of λ. As discussed above, the quantitative precision of the approximate techniques may be extended to the case $\epsilon=0$.

The origin of the θ vacuum in Yang-Mills field theory[20] is the same as that in our simple quantum-mechanical model, i.e., the topology of the configuration space is multiply connected in both cases. It would be extremely interesting to find out if there exists in field theory any analogy with the phenomena we have observed in the planar rotor, such as the vacuum degeneracy, and its implications.

Among the approximate methods we have used here, only two of them are currently used in field theory: the instanton method and the Monte Carlo method (this one in connection with the lattice strategy). From the experience gained with the rotor, one should think that instantons provide accurate qualitative results only in its natural range of validity. On the other hand, the Monte Carlo method, with enough computer time, is more flexible and provides qualitative agreement for any value of the coupling constant. Finally, we would like to remark that it is a pity not to possess in field theory something equivalent to the variational method of quantum mechanics; any serious attempt in this direction would be highly welcomed.

ACKNOWLEDGMENTS

We would like to acknowledge the I.F.N.A.E. and J.E.N. for partial financial support.

[1]J. D. Bjorken, in *Quantum Chromodynamics,* proceedings of the Summer Institute on Particle Physics, SLAC, 1979, edited by Anne Mosher (SLAC, Stanford, 1980); R. Jackiw and C. Rebbi, Phys. Rev. Lett. 37, 178 (1976); C. Callan, R. Dashen, and D. Gross, Phys. Lett. 63B, 334 (1976).

[2]S. Coleman, in *The Whys of Subnuclear Physics,* proceedings of the International School of Subnuclear Physics, Erice, 1977, edited by A. Zichichi (Plenum, New York, 1979).

[3]G. 't Hooft, Phys. Rev. D 14, 3432 (1976).

[4]K. G. Wilson, Phys. Rev. D 10, 2445 (1974); M. Creutz, *ibid.* 21, 2308 (1980); Phys. Rev. Lett. 45, 313 (1980).

[5]C. C. Lin and J. D. Swalen, Rev. Mod. Phys. 31, 841 (1959).

[6]M. Peshkin, Phys. Rev. A 23, 360 (1981).

[7]Y. Aharonov and D. Bohm, Phys. Rev. 115, 485 (1959); M. Asorey and L. J. Boya, Int. J. Theor. Phys. 18, 295 (1979).

[8]P. Bocchieri and A. Loinger, Nuovo Cimento A47, 475 (1978).

[9]D. Bohm and B. J. Hiley, Nuovo Cimento 52, 295 (1979).

[10]C. DeWitt-Morette, A. Maheshwari, and B. Nelson, Phys. Rep. 50, 255 (1979).

[11]*Handbook of Mathematical Functions,* edited by M. Abramowitz and I. A. Stegun, (Dover, New York, 1972), p. 721; S. Flugge, *Practical Quantum Mechanics* (Springer, Berlin, 1971), Vol. III, p. 43.

[12]C. Schwartz, Ann. Phys. (N.Y.) 32, 277 (1965).

[13]S. J. Chang, Phys. Rev. D 12, 1071 (1975).

[14]For an excellent review on the use of instantons see Ref. 2, p. 805.

[15]We use $0 \leq \arctan x \leq \pi$.

[16]R. P. Feynman and A. R. Hibbs, *Quantum Mechanics and Path Integrals* (McGraw-Hill, New York, 1965).

[17]N. Metropolis, A. Rosenbluth, M. Rosenbluth, A. Teller, and E. Teller, J. Chem. Phys. 21, 1087 (1953); K. Binder, in *Phase Transitions and Critical Phenomena,* edited by C. Domb and M. S. Green (Academic, New York, 1976); M. Creutz and B. Freedman, Ann. Phys. (N.Y.) 132, 427 (1981).

[18]The numbers for Δ and a which appear in Table II have been chosen according to (6.14). We shall notice that the results one gets for E_0 are pretty independent of the value of those parameters.

[19]T. Kato, *Perturbation Theory for Linear Operators* (Springer, New York, 1966).

[20]M. Asorey and P. K. Mitter, CERN Report No. TH3424, 1982 (unpublished).